UKACC International Conference on Control 2012
Cardiff, UK, 3-5 September 2012

Experimental validation of a geometric method for the design of stable and broadband vibration controllers using a propeller blade test rig

Ubaid Ubaid*, Steve Daley†, Simon Pope*, Ilias Zazas†
*Automatic Control and Systems Engineering, University of Sheffield, S1 3JD, UK.
†Institute of Sound and Vibration Research, University of Southampton, SO17 1BJ, UK.

***Abstract*—A systematic geometric design methodology to generate a stable controller for simultaneous local and remote attenuation that was previously proposed is experimentally validated on a structure. The local control path transfer function for this experimental system is non-minimum phase due to which the original broadband controller design would yield an unstable controller. Here a modified procedure for systems with local non-minimum phase dynamics is used to generate a stable controller. According to this method, reduction in vibration at local and remote points on a structure can be parameterised in terms of the available design freedom and a controller is realised in terms of the optimal selection of this using the minimum phase counterpart of the local control path transfer function. The modified method results in a controller that is both stable and stabilizing and which achieves the desired vibration attenuation at the local and remote points on the structure. An experimental facility that replicates the vibration transmission through the shaft of a propeller blade rig system is used to demonstrate the method. Vibration for excitation near the first bending mode frequency of the resonating part of this structure is attenuated at the non-resonating part of the system without deteriorating vibration at the resonating end.**

I. Introduction

Active control for reduction of vibration at a specific point on a complex interconnected structure can potentially enhance vibration at other points on the structure [1]. A controller design technique to address the vibration attenuation problem at local and remote points on a structure simultaneously using only a single locally placed sensor actuator pair was presented for a discrete frequency excitation case in [2] and later extended for the broadband case [3]. For vibration attenuation over an arbitrary frequency band, controller implementation involves inversion of the local control path transfer function. When the local control path transfer function is non minimum phase, then the controller itself would be unstable. This problem can be solved using a new design freedom [4] to parameterise reduction in vibration at local and remote points whereby the controller is implemented in terms of the minimum phase counterpart of the local control path transfer function. Additionally, to improve robustness to unmodelled high frequency dynamics, a filter is incorporated into the design freedom selection [5] such that the gain of the closed loop system rolls off at high frequency without deteriorating controller performance in the excitation frequency bandwidth. The aim of this paper is to present experimental verification of this design technique for attenuation of vibration at both local and remote points on a blade rig simultaneously. Trade-offs between stability robustness and disturbance attenuation are also highlighted in terms of the values of the design freedom parameter.

II. Experimental set-up

A schematic diagram of the blade rig is shown in figure 1. The primary excitation signal $f_p(t)$ is a common signal fed to the two smaller shakers attached at both ends of the bar which acts as the transient loading force due to rotation of the propeller blades. The vibration at the blade end of the shaft $q_p(t)$ is the summation of outputs measured by two accelerometers connected near each of the disturbance shakers. The control input $f_c(t)$ is applied to the control shaker attached at the other end of propeller shaft on the thrust block and a local accelerometer on the thrust block measures local vibration levels $q_c(t)$. Vibration is transmitted from the blade end along the shaft to the thrust block end and is particularly detrimental at the blade resonant frequency. Due to difficulties in measuring and actuating at the blade end for most applications, it is desired to control both blade vibration and its transmission using sensors and actuators placed at the thrust block only[1]. This blade system can be considered as a two input two output system with the transfer function matrix relating the disturbance and control inputs to the remote and local vibration outputs as

$$\begin{bmatrix} q_c(j\omega) \\ q_p(j\omega) \end{bmatrix} = \begin{bmatrix} g_{cc}(j\omega) & g_{cp}(j\omega) \\ g_{pc}(j\omega) & g_{pp}(j\omega) \end{bmatrix} \begin{bmatrix} f_c(j\omega) \\ f_p(j\omega) \end{bmatrix} \quad (1)$$

In the next section, a design freedom parameter is introduced which parameterizes reduction in vibration at the thrust block and blade end. A controller implemented in terms of the optimally selected values of this design freedom would achieve the targeted vibration reduction.

III. General algorithm

The detailed synthesis of a stable controller using the geometric approach is given in [4], [5]. For the system described in (1), the aim is to design a feedback controller $k(j\omega)$ using as feedback signal only from the thrust block to achieve vibration

[1]Note that this general concept is the subject of several BAE Systems patents

978-1-4673-1558-6/12/$31.00 ©2012 IEEE

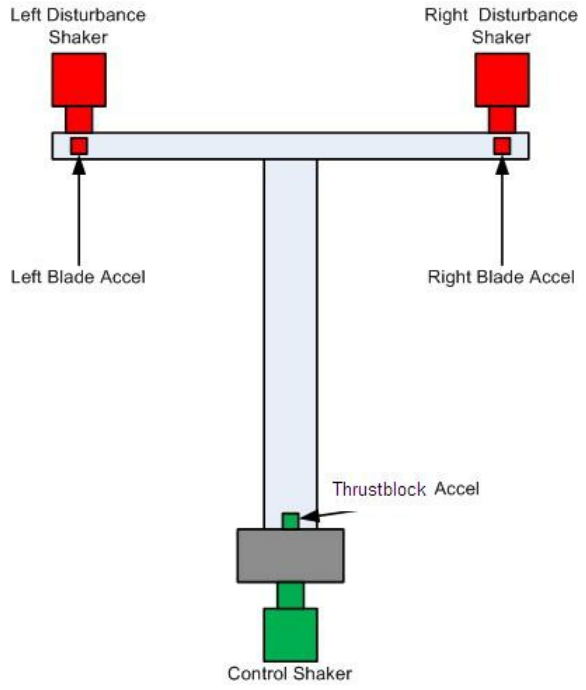

Figure 1. Schematic of blade rig

reduction at both the thrust block and blade end simultaneously. Using control action, $f_c(j\omega) = -k(j\omega)q_c(j\omega)$, the closed loop output respectively at the local and remote points is then given as

$$q_c(j\omega) = \left[1 + \frac{-g_{cc}(j\omega)k(j\omega)}{1 + g_{cc}(j\omega)k(j\omega)}\right] g_{cp}(j\omega)f_p(j\omega) \quad (2)$$

and

$$q_p(j\omega) = \left[1 + \frac{-g_{cc}(j\omega)k(j\omega)}{1 + g_{cc}(j\omega)k(j\omega)} \frac{g_{cp}(j\omega)g_{pc}(j\omega)}{g_{cc}(j\omega)g_{pp}(j\omega)}\right] g_{pp}(j\omega)f_p(j\omega) \quad (3)$$

Denote a design freedom parameter γ which is related to the sensitivity function $S(j\omega)$ as

$$\gamma(j\omega) = \frac{1}{g_{AP}(j\omega)f_{LP}(j\omega)} [S(j\omega) - 1] \quad (4)$$

where $g_{AP}(j\omega)$ is the all pass transfer function formed from the right half plane zeros of $g_{cc}(j\omega)$ and $f_{LP}(j\omega)$ is a low pass or a bandpass filter which improves robustness at out-of-band frequencies. The closed loop local and remote outputs in (2) and (3) can be represented in terms of this parameter variable as

$$q_c(j\omega) = [1 + \gamma(j\omega)g_{AP}(j\omega)f_{LP}(j\omega)]\, g_{cp}(j\omega)f_p(j\omega) \quad (5)$$

and

$$q_p(j\omega) = \left[1 + \gamma(j\omega)g_{AP}(j\omega)f_{LP}(j\omega)\frac{g_{cp}(j\omega)g_{pc}(j\omega)}{g_{cc}(j\omega)g_{pp}(j\omega)}\right] g_{pp}(j\omega)f_p(j\omega) \quad (6)$$

The magnitude of the expression inside brackets in RHS of (5) and (6) determines reduction in closed loop local and remote output. The magnitude of these terms can be represented as

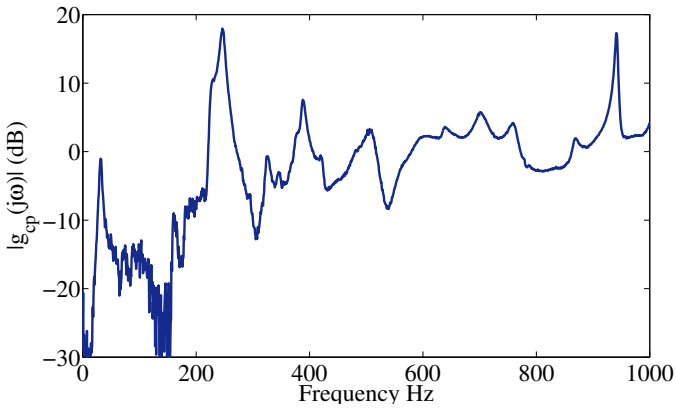

Figure 2. Measured frequency response of primary excitation input to thrust block vibration output

a circle at each discrete frequency in a $\gamma-$plane. A value for γ from inside the circle corresponds to reduction in vibration. If values for γ at discrete frequencies in the disturbance frequency bandwidth $[\omega_L, \omega_H]$ is selected from inside the circles given by inequalities (7) and (8), then reduction in vibration at the local and remote points is possible.

$$\left|\gamma(j\omega_i) + \frac{1}{g_{AP}(j\omega_i)f_{LP}(j\omega_i)}\right| < \left|\frac{1}{g_{AP}(j\omega_i)f_{LP}(j\omega_i)}\right| \quad (7)$$

$$\left|\gamma(j\omega_i) + \frac{1}{g_{AP}(j\omega_i)f_{LP}(j\omega_i)} \frac{g_{cc}(j\omega)g_{pp}(j\omega)}{g_{cp}(j\omega)g_{pc}(j\omega)}\right| < \left|\frac{1}{g_{AP}(j\omega_i)f_{LP}(j\omega_i)} \frac{g_{cc}(j\omega)g_{pp}(j\omega)}{g_{cp}(j\omega)g_{pc}(j\omega)}\right| \quad (8)$$

These optimal γ points are interpolated by a stable transfer function and the controller is implemented as

$$k(j\omega) = -\frac{\gamma(j\omega)f_{LP}(j\omega)}{[1 + \gamma(j\omega)g_{AP}(j\omega)f_{LP}(j\omega)]g_{MP}(j\omega)} \quad (9)$$

where $g_{MP}(j\omega)$ is the minimum phase counterpart of the local control path transfer function.

The magnitude frequency response of the open loop path from primary excitation input on the blade to the local and remote outputs, denoted as $g_{cp}(j\omega)$ and $g_{pp}(j\omega)$ respectively, is plotted in figures 2 and 3. It shows that near the frequency of the first bending mode of the blade (i.e. the iron bar connected to one end of the shaft), vibration transmission to the thrust block is amplified. A feedback controller to achieve simultaneous reduction in the thrust block and blade vibration outputs will be designed for primary excitation around this frequency range.

The first step in controller design is to determine an LTI model for the open loop control path $g_{cc}(j\omega)$ from the measured FRF. As the controller will target vibration reduction in the low frequency region, the measured FRF of the path from control shakers to acceleration on thrust block at frequencies below 800 Hz is fitted with a 15^{th} order transfer function model using least squares. The dynamics neglected at frequencies higher than 800 Hz will not be a problem as they will not be excited by the control action due to low pass

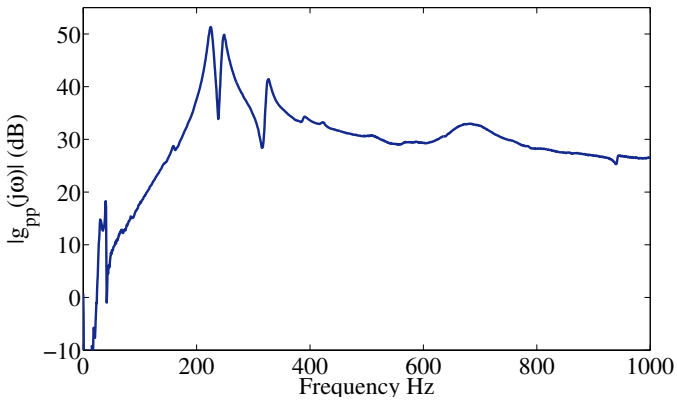

Figure 3. Measured frequency response of primary excitation input to blade vibration output

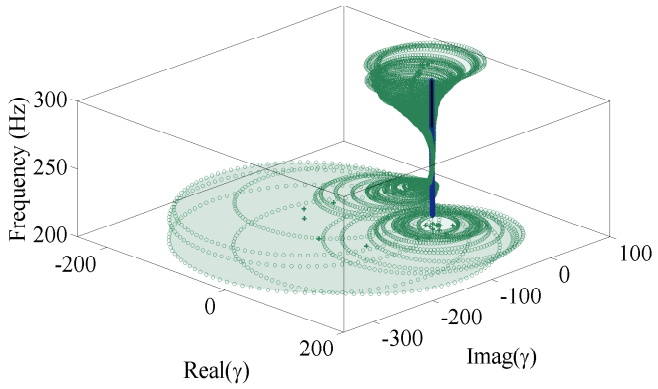

Figure 4. Circles that represent remote vibration attenuation in $\gamma-$ plane at discrete frequencies between 200 Hz and 300 Hz. Unit radius circles corresponding to local vibration attenuation appear as a cylinder that passes through the origin

filter $f_{LP}(j\omega)$. This identified transfer function has 1 right half plane zero so that $g_{AP}(j\omega)$ is of order 1 and $g_{MP}(j\omega)$ has this RHP zero reflected into the LHP.

The circles in the $\gamma-$plane corresponding to reduction in vibration at the local and remote outputs given by (7) and (8) for frequencies around the first bending mode is shown in figure 4. The circles corresponding to reduction in vibration at the blade end are very large in the frequency region from 200 Hz to 220 Hz and above 270 Hz. The distance between the centre of both circles will be large and so it will not be possible to achieve considerable vibration reduction at the blade end without amplifying vibration output at the thrust block end. Optimal γ points at these frequencies are selected such that the vibration level at the thrust block is reduced without enhancing the vibration level at the blade end. $f_{LP}(j\omega)$ is chosen as a bandpass filter with lower and higher cut-off frequency as 100 Hz and 600 Hz, respectively.

IV. Nevanlinna-Pick interpolation

The set of selected optimal γ points at discrete frequencies in the disturbance frequency bandwidth is interpolated by a stable transfer function using the Nevanlinna Pick interpolation algorithm [6]. This interpolation problem can be stated as follows: given n distinct points $s_1, \ldots, s_n$ in the right half plane Π^+ and a collection of complex numbers $H_1, \ldots, H_n$, determine a transfer function $f(s)$ that is analytic in Π^+ with

$$\sup |f(s)| \leq 1$$

such that $f(s_i) = H_i$, for all $i = 1, \ldots, n$. The solution of this interpolation exists if and only if the associated Pick matrix P

$$P = \left[\frac{1 - H_k \overline{H}_l}{s_k + \overline{s}_l}\right]_{k,l=1}^{n}$$

is positive definite, where $\overline{\bullet}$ denotes complex conjugate. The points s_i according to the above theorem should strictly belong to the Right Half Plane, whereas the set of optimal selected values for the design freedom γ have to be interpolated on the imaginary $j\omega$ axis. The frequency points are shifted into the RHP using transformation of Lemma 2 in [8] and is stated as follows: for the optimal γ data values at n discrete frequencies ω_i, for $i = 1, \ldots, n$, a stable transfer function $\gamma(j\omega)$ exists if and only if the associated Pick matrix

$$P = \left[\frac{1 - W_k \overline{W}_l}{s_k + \overline{s}_l}\right]_{k,l=1}^{n} \tag{10}$$

is positive definite, where $W_i = \gamma_i / M$ and $s_i = \sigma + j\omega_i$, for $i = 1, \ldots, n$. where M is the maximum modulus of interpolated transfer function and σ a positive real number. Increasing M or decreasing σ increases the positive definitness of the pick matrix but for a stable controller and good performance at intermediate frequencies, M and σ values have to be finely tuned. It should be noted that small values of σ will give interpolated transfer function $\gamma(j\omega)$ with poles that are close to the imaginary axis. This would cause oscillations in the frequency response of the identified transfer function $\gamma(j\omega)$ leading to gain and phase crossover at intermediate frequencies. As the non-interpolated points in the disturbance frequency band for small values of σ may lie outside (7) and (8) circles in $\gamma-$plane, this would deteriorate controller performance. Although large value of σ gives better approximation at intermediate frequencies, M values will have to be increased to get a positive definite pick matrix. A large value of M can result in the nyquist contour of $\gamma(j\omega)g_{AP}(j\omega)f_{LP}(j\omega)$ encircling the critical point which will cause the controller to become unstable as can be seen from (9). If the Pick matrix (10) of optimally selected γ points is not positive definite, then an approximate set of sub-optimal points adjusted to lie inside the circles is obtained using Linear Matrix Inequalities that also satisfy the pick condition. This new set of γ points is used to obtain the interpolating function using the classical N-P interpolation algorithm.

The first step in iterative classical N-P interpolation algorithm is to compute the elements of Fenyves array T.

$$T_{k,l} = \frac{s_l + \bar{s}_{k-1}}{s_l - s_{k-1}} \frac{T_{k-1,l} - T_{k-1,k-1}}{1 - T_{k-1,l}\overline{T}_{k-1,k-1}} \qquad 2 < k < n,\ k < l < n \tag{11}$$

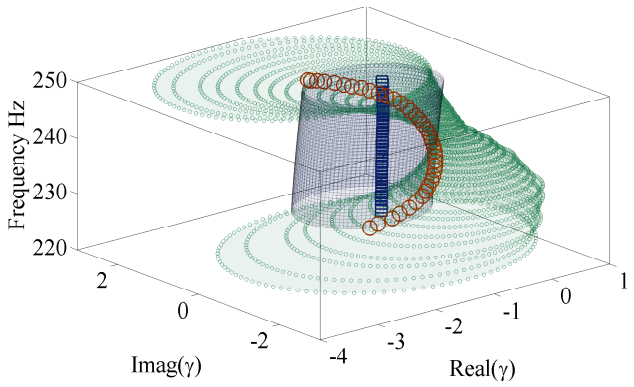

Figure 5. Final operating γ points as the frequency response of a stable bounded real interpolated transfer function $\gamma(j\omega)$

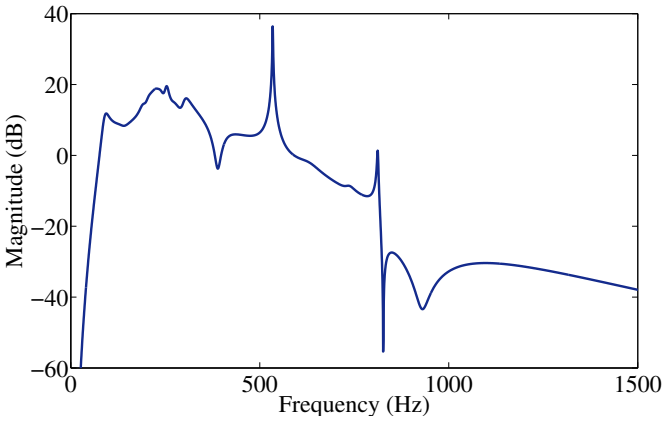

Figure 6. Magnitude plot of the frequency response of controller

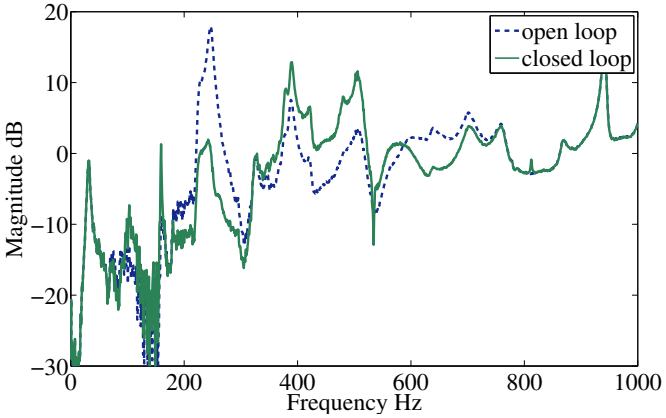

Figure 7. Magnitude plot of the frequency reponse from disturbance to local output with (dashed) and without (solid) feedback controller

where $T_{1,l} = W_l$, for $1 < l < n$. The next step is to recursively estimate $W_1(s)$ from

$$W_k(s) = \frac{T_{k,k} + W_{k+1}(s)\frac{s-s_k}{s+\bar{s}_k}}{1 + \overline{T}_{k,k} W_{k+1}(s)\frac{s-s_k}{s+\bar{s}_k}}, \qquad k = n, n-1, \ldots, 2, 1 \tag{12}$$

If the set of data points (s_i, W_i) for interpolation is augmented with its complex conjugate $(\bar{s}_i, \overline{W}_i)$, then a stable bounded real analytic interpolating function is given by $\gamma(s) = M \times \frac{1}{2}\left[W_1(s+\sigma) + \overline{W}_1(s+\sigma)\right]$ for any arbitrarily selected initial stable bounded analytic function $W_{k+1}(s)$ in (12). There will be at least 4 poles and zeros in $\gamma(j\omega)$ transfer function for every interpolated γ point which will affect the order of the final compensator transfer function $k(j\omega)$. In the frequency interval from 200 Hz to 300 Hz there are 164 discrete frequencies at which an optimal γ point is selected. Only 6 of the optimal γ points are used as interpolation data points in order to get a lower order controller.

The final operating γ points obtained from the frequency response of the interpolating function $\gamma(j\omega)$ for frequency 225 Hz to 250 Hz is shown in figure 5. It is seen that in the frequency range 230 Hz to 245 Hz, circles representing remote vibration reduction converge towards the origin and become very small. Due to this several more optimal γ points have to be selected in this frequency band alone to get a good transfer function approximation, but this will increase the order of interpolated transfer function considerably. At all other frequencies in the disturbance frequency band, circles representing reduction in vibration at the remote point are considerably larger than the unit circle that corresponds to local vibration attenuation. Hence, final operating γ points from inside the unit circle will lie on the boundary of the remote vibration reduction circle. This is predicted to achieve only slight reduction in the blade vibration output using a 58^{th} order controller transfer function. This vibration attenuation problem is a case of very extreme magnitude for the dimensionless parameter discussed in [7], which is equivalent to the function formed by the centre of remote vibration reduction circle given as $-g_{cc}(j\omega)g_{pp}(j\omega)\left[g_{cp}(j\omega)g_{pc}(j\omega)g_{AP}(j\omega)f_{LP}(j\omega)\right]^{-1}$. The magnitude of this function is a measure of the severity of the trade-off between disturbance attenuation and stability robustness.

A controller realized in terms of this $\gamma(j\omega)$ transfer function by substituting in (9) has a magnitude frequency spectrum as shown in figure 6. The gain of controller starts to roll-off at 600 Hz due to the filter action thereby improving robustness to unmodelled high frequency dynamics. The theoretical closed loop frequency response of local and remote points with the designed controller is compared with the open loop frequency response as shown in figures 7 and 8.

V. Experimental Results

The controller obtained in the previous section is a compensator transfer function in continuous time domain. It is integrated with the experimental set-up through Simulink using a dSPACE real time interface prior to which it has to be converted to a discrete time model. A discrete model of compensator using first order hold method with a sampling frequency of 5 kHz is obtained which matches exactly the frequency characteristic of the continuous time domain compensator in the disturbance frequency bandwidth. For different primary excitation inputs $f_p(t)$, the acceleration output at the thrust block $q_c(t)$ and blade end $q_p(t)$ are measured to compare closed loop output against open loop output.

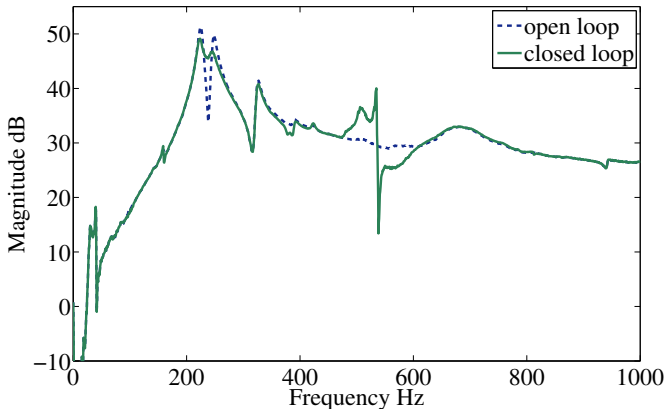

Figure 8. Magnitude spectrum of the frequency reponse from disturbance to remote output with (dashed) and without (solid) feedback controller

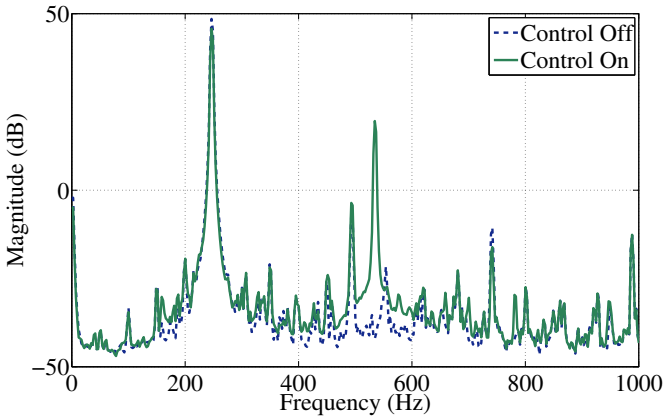

Figure 10. Power spectral density of output from blade end when primary excitation is discrete frequency excitation at 247 Hz

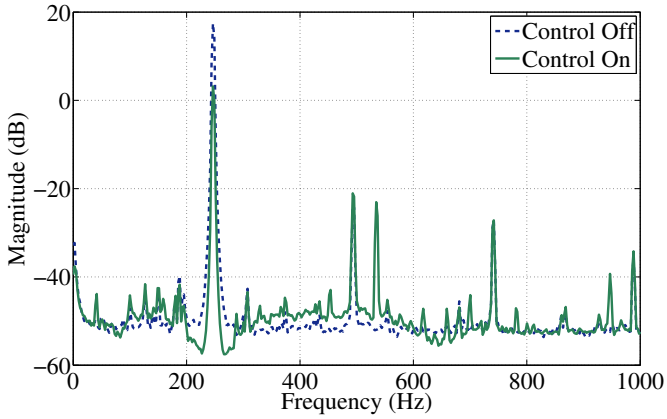

Figure 9. Power spectral density of output from thrust block when primary excitation is discrete frequency excitation at 247 Hz

A. Sinusoidal excitation at discrete frequency 247 Hz

The power spectral density of measured acceleration at the thrust block with and without feedback control for a primary excitation signal at 247 Hz is plotted in figure 9. It shows more than 14 dB reduction in magnitude at 247 Hz using feedback controller and the power spectral density of measured acceleration at the blade end in figure 10 shows around 3 dB reduction in magnitude at 247 Hz. A peak at 534 Hz in the PSD of both closed loop outputs can be noticed which is not present for the open loop case. This is caused by the peak at this frequency in the magnitude of controller frequency response spectrum. In the next section, this peak is reduced without affecting controller performance in the design frequency bandwidth using a notch filter.

VI. Results after augmenting a notch filter

The controller implementation involves inversion of the minimum phase counterpart of the local control path transfer function so an antiresonance at frequency 534 Hz in the local control path transfer function appears as a peak in the controller FRF. Filter $f_{LP}(j\omega)$ has a high cut-off frequency 600 Hz which is higher than the frequency (534 Hz) at which the peak in controller FRF appears. If the high cut-off frequency of $f_{LP}(j\omega)$ is reduced below 534 Hz and the order of filter is increased in order to take account of the sharp increase in this peak then due to limitations as quantified by Bode's sensitivity integral, amplification at out-of bound frequencies will not be spread over a large frequency range and there will be peaks appearing in the closed loop frequency response. Therefore, the controller is implemented in series with a notch filter which has a notch at 534 Hz in order to reduce the peak at this frequency. The magnitude and phase of the controller is unaffected in the disturbance frequency bandwidth. The acceleration measurements at the thrust block and blade end are taken for different disturbance excitation signals to compare reduction in closed loop output.

A. Sinusoidal excitation at discrete frequency 247 Hz

The power spectral density of acceleration measured at the thrust block with and without feedback control for a primary excitation signal at 247 Hz shows 16 dB reduction in magnitude as shown figure 11. The power spectral density of acceleration measured at the blade end in figure 12 shows around 3 dB reduction in magnitude at 247 Hz. The peak at 534 Hz is reduced considerably because of the notch filter at this frequency.

B. Broad band frequency white noise excitation

The primary excitation signal input to the disturbance shaker is a random white noise signal and the power spectral density of acceleration outputs from the thrust block $q_c(t)$ and blade end $q_p(t)$ with and without feedback control action is plotted in figures 13 and 14. The PSD of acceleration measured at the thrust block shows around 12 dB attenuation in the disturbance frequency bandwidth while the PSD of measured blade acceleration shows no amplification and a small attenuation as designed.

VII. Conclusion

A geometric design methodology for vibration control using remotely located stable control systems has been demonstrated

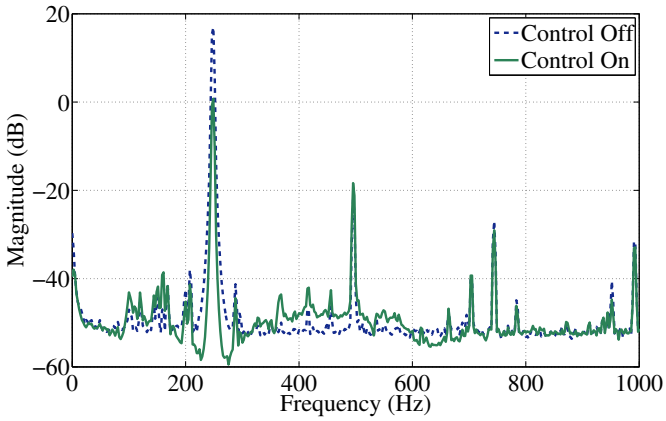

Figure 11. Power spectral density of output from thrust block when primary excitation is discrete frequency excitation at 247 Hz

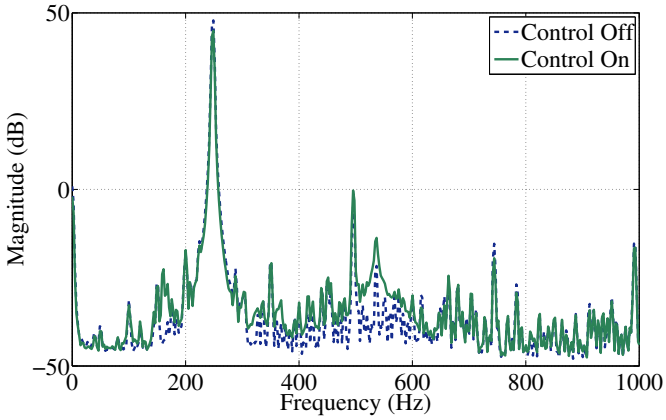

Figure 12. Power spectral density of output from blade end when primary excitation is discrete frequency excitation at 247 Hz

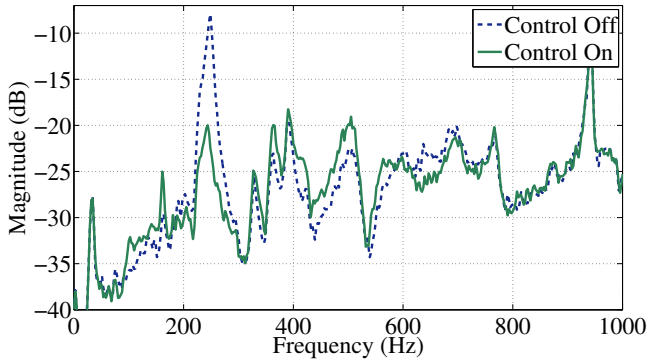

Figure 13. Power spectral density of output at thrust block with primary excitation as random white noise excitation

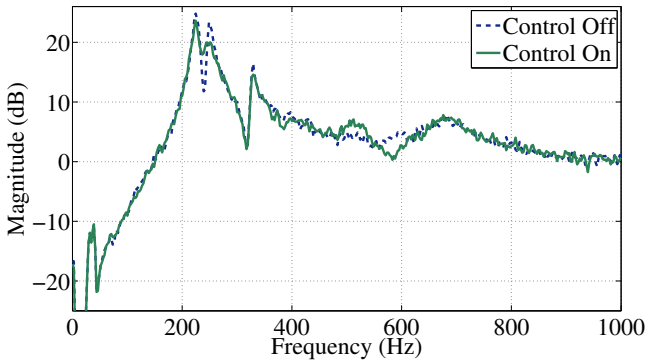

Figure 14. Power spectral density of output at blade end with primary excittion as random white noise excitation

experimentally on a blade rig experimental set-up, which mimicks the vibration transmission problems encountered due to propeller blade excitations encountered in many aerospace and maritime applications. The limitations on actuator and sensor placement can be overcome using this control design approach and shows considerable reduction in closed loop output at the thrust block side near the problematic blade resonant frequency.

REFERENCES

[1] J. Post and R. Silcox, *Active control of the forced response of a finite beam*, Noise Control Engineering Journal, 1 (1990), pp. 197-202.

[2] S. Daley and J. Wang, *A geometric approach to the design of remotely located vibration control systems*, Journal of Sound and Vibration, 318 (2008), pp. 702-714.

[3] J. Wang and S. Daley, *Broad band controller design for remote vibration using a geometric approach*, Journal of Sound and Vibration, 329 (2010), pp. 3888-3897.

[4] U. Ubaid, S. Daley and S. Pope, *Broad band design of remotely located vibration control systems: a stable solution for non-minimum phase dynamics*, Internoise 2011, Osaka, Japan, September 4-7 2011.

[5] U. Ubaid, S. Daley and S. Pope, *Design of remotely located stable vibration controllers for non-minimum phase systems*, in 14th Asia Pacific Vibration Conference, Hong Kong, December 5-8 2011.

[6] Ph. Delsarte, Y. Genin and Y. Kamp, *The Nevanlinna-Pick problem for matrix-valued functions*, SIAM Journal on Applied Mathematics, Vol. 36, 1 (1979), pp. 47-61.

[7] J. Freudenberg, C. Hollot and R. Middleton, *A tradeoff between disturbance attenuation and stability robustness*, in American Control Conference, 2003. Proceedings of, vol. 6, IEEE, 2003, pp. 4816-4821.

[8] G. Ferreres and G. Puyou, *Feasibility of H∞ design specifications: an interpolation method*, International Journal of Control, 78 (2005), pp. 927-936.